Contrib Mineral Petrol (1996) 126: 51–66

Sharon N. Feldstein · Rebecca A. Lange
Torsten Vennemann · James R. O'Neil

Ferric-ferrous ratios, H_2O contents and D/H ratios of phlogopite and biotite from lavas of different tectonic regimes

Received: 5 January 1995 / Accepted: 19 March 1996

Abstract Complete chemical analyses, including ferric and ferrous iron, H_2O contents and dD values for 16 phlogopite and biotite and 2 hornblende separates are presented. Samples were obtained from volcanic rocks from four localities: (1) phlogopite phenocrysts from minette lavas from the western Mexico continental arc, (2) biotite and hornblende phenocrysts from andesite lavas from Mono Basin, California, (3) phlogopite and biotite from clinopyroxenite nodules entrained in potassic lavas from the East African Rift, Uganda, and (4) phlogopite phenocrysts from a wyomingite lava in the Leucite Hills, Wyoming. The Fe_2O_3 contents in the micas range from 0.8 to 10.5 wt%, corresponding to 0.09 to 1.15 Fe^{3+} per formula unit (pfu). Water contents vary from 1.6 to 3.0 wt%, corresponding to 1.58 to 3.04 OH pfu, significantly less than would be expected for a site fully occupied by hydroxyl. Cation- and anion-based normalization procedures provide accurate mineral formulae with respect to most cations and anions, but are unable to generate accurate estimates of Fe^{3+}/Fe^{T}, and overestimate OH at the expense of O on the hydroxyl site. These inaccuracies are present despite acceptable adjusted totals and stoichiometric calculated site occupancies. The phlogopite and biotite phenocrysts in arc-related lavas from western Mexico and eastern California have the highest Fe^{3+}/Fe^{T} ratios (56–87%), reflecting high magmatic oxygen fugacities (DNNO = +2 to +5), in contrast to those from Uganda (25–40%) and the Leucite Hills (23%). There is no correlation between the OH content and the Fe^{3+}/Fe^{T} ratio in the micas. Values of $K_D^{Mg/Fe^{2+}}$ (+ 2s errors) were calculated for three phlogopite-olivine pairs (0.12 + 0.12, 0.26 + 0.14, 0.09 + 0.12), two biotite-hornblende pairs (0.73 + 0.08 and 1.22 + 0.10) and a single phlogopite-augite pair (1.15 + 0.12). Values of $K_D^{F/OH}$ for two biotite and hornblende pairs could not be determined without significant error because of the extremely low F contents (< 0.2 wt%) of the four phases. The dD values obtained in this study encompass a large range (−137 to −43‰). The phlogopite and biotite separates from Uganda have dD values of −70 to −49‰, which overlap those believed to represent "primary" mantle. There is a larger range in dD values (−137 to −43‰) for phlogopite phenocrysts from western Mexico minette lavas, although their range in $d^{18}O$ values (5.2–6.2‰) is consistent with "normal" mantle. It is unlikely, therefore, that the variable dD values reflect heterogeneity in the mantle source region of the minette magmas. Nor can the extremely low dD values reflect degassing of H_2 or H_2O since almost 100% loss of dissolved water in the magma is required, an unrealistic scenario given the stability of the hydrous phenocrysts. The very low dD values of the Mascota minette phlogopites require that the hydrogen be introduced from an external source (e.g., meteoric water). Whatever the process responsible for the observed hydrogen isotope composition, it had no effect on the $d^{18}O$ value, f_{O_2}, a_{H_2O} or bulk composition of the host magmas.

S. N. Feldstein (✉) · R. A. Lange · T. Vennemann · J. R. O'Neil
Department of Geological Sciences, University of Michigan, Ann Arbor, MI 48109, USA

T. Vennemann
Institut für Geochemie, Wilhelmstrasse 56, D-72074 Tübingen, Germany

Editorial responsibility: T. Grove

Introduction

Phlogopite and biotite are common phenocryst phases in many volcanic rocks, including andesites, dacites, rhyolites, as well as potassic and ultrapotassic varieties such as minettes, kersantites and lamproites. Phlogopite and biotite can be used to evaluate magmatic f_{O_2} and f_{H_2O} because these minerals contain both ferric and ferrous iron and a variable number of hydroxyl ions in their structure. The incorporation of ferric iron into the phlogopite-biotite solid solution can occur as the oxyannite component, $KFe^{2+}Fe_2^{3+}AlSi_3O_{12}$, as well as other components such as $KMgFe_2^{3+}AlSi_3O_{12}$. The amount of oxygen substituting for hydroxyl ions, however, is not necessarily correlated with ferric iron (and hence

with f_{O_2}) because of other components such as $KMgAl_2AlSi_3O_{12}$ and $KMg_2TiAlSi_3O_{12}$.

The use of phlogopite and biotite to determine magmatic intensive variables requires the development of an activity-composition model for mica solid solutions, which is well beyond the scope of this study. One of the limiting factors to the development of such a model is the general paucity of complete chemical analyses of micas. Most are analyzed with the electron microprobe, which cannot distinguish between ferric and ferrous iron or measure H_2O contents directly. The result is the dependence on some normalization scheme for an estimate of ferric iron and hydroxyl concentrations. The problems inherent in generating a mineral formula for micas from microprobe data alone have long been recognized (Bohlen et al. 1980; Holdaway 1980; Dymek 1983; Hewitt and Abrecht 1986; Afifi and Essene 1988; Dyar et al. 1991; Schumacher 1991).

In order to use phlogopite and biotite phenocrysts to infer pre-eruptive magmatic conditions, it is clearly advantageous to study separates from fresh volcanic rocks rather than from plutonic rocks. Because of the rapid cooling in the volcanic environment, subsolidus re-equilibration is minimized. Moreover, mineral alteration associated with interaction with meteoric water, important in the development of many intrusions (Taylor 1977; Criss and Taylor 1986), is normally non-existent in phenocrysts of young lavas. Unfortunately, few complete chemical analyses (including FeO, Fe_2O_3 and H_2O) of phlogopite and biotite phenocrysts from volcanic rocks are published in the recent literature. Instead, one must look to papers published prior to the advent of the electron microprobe to find a significant number of complete chemical analyses (e.g., Doelter 1917; Winchell 1935; Nockolds 1947; Foster 1960; Deer et al. 1962). Many of these complete analyses, however, have poor totals or recalculate to nonstoichiometric mineral formulae, with excess cations on the octahedral and interlayer sites, and/or excess H_2O, consistent with alteration of the micas or impure separates. Another possible factor in the poor calculated mineral stoichiometry and low totals is the absence of BaO, SrO, F and Cl determinations in most of these analyses.

Although most recent published analyses of phlogopite and biotite are not complete, some include ferric-ferrous ratios without wt% H_2O or wt% H_2O without ferric-ferrous ratios; the latter are usually part of studies of the D/H variation of hydrous rocks and minerals. Recently, significant effort has been made to obtain ferric and ferrous iron analyses of metamorphic biotites by Mössbauer spectroscopy (Dyar and Burns 1986; Dyar 1988, 1990; Guidotti and Dyar 1991), and ferric-ferrous analyses of phlogopite phenocrysts in lamprophyric lavas by wet chemical methods (Wallace and Carmichael 1989; Lange and Carmichael 1991). Although these data provide some information on the range of ferric-ferrous ratios found in phlogopite and biotite, correct mineral formulae cannot be determined without accurate determination of wt% H_2O as well.

In light of these problems, the goal of this study is to provide a data base of complete chemical analyses, including ferric and ferrous iron, H_2O contents and dD values for phlogopite and biotite in lavas from different tectonic environments. These data will be examined to determine whether variations in the ferric-ferrous ratios, O and H_2O contents, and dD values of phlogopite and biotite have been altered by processes such as degassing and post-eruptive oxidation, or reflect pristine magmatic values. In cases where the compositions of the phlogopite and biotite samples are pristine, these data will be used to evaluate any correlation between the ferric-ferrous ratio and hydroxyl content and the tectonic environment of their host volcanic rock. In addition, Mg-Fe^{2+} exchange equilibria between phlogopite-clinopyroxene, biotite-hornblende and phlogopite-olivine phenocryst pairs, and F-OH exchange equilibria between biotite-hornblende phenocryst pairs will be calculated.

Tectonic setting of host rocks

The phlogopite, biotite and hornblende samples used in this study were obtained from a variety of lavas from different tectonic settings. Most are phenocrysts with the exception of the phlogopite and biotite grains from the xenoliths from Uganda, Africa.

The continental arc of western Mexico

Phlogopite phenocrysts were separated from five different Quaternary minette lavas from the western Mexico continental arc (Luhr et al. 1989). Four samples (Mas-3a, -4, -11, and -18) are from separate lava and cinder cones from the Mascota volcanic field described by Carmichael et al. (1996). A fifth sample is from a lava flow near the town of San Sebastian, ¥20 km north of Mascota (Lange and Carmichael 1991). Mas-4 is a rapidly quenched scoria whereas all other samples are from flows. The phenocryst assemblage of these five minette lavas is phlogopite + augite + olivine. All samples erupted between 69 and 489 ka and are unaltered (Lange and Carmichael 1991; Carmichael et al. 1996). Petrologic and trace element data are consistent with the derivation of the minette magmas from a phlogopite-bearing mantle source that formed through hydrous enrichment of the subarc lithosphere in response to subduction (Wallace and Carmichael 1989).

Andesite volcanism near Mono Basin, California

Biotite and hornblende phenocryst pairs were separated from two andesite lavas (SN-31 and -161) that erupted ¥10 km north of Mono Basin in east-central California. The two lava flows are part of a broad volcanic field that has been active over the last 4 milliion years in which ¥100 km^3 of potassium-rich basaltic through andesitic magmas erupted over 400 km^2 extending from the margins of the Mono Basin, the periphery of Long Valley caldera, and southwestward into the Sierra Nevada (Lange et al. 1993). The trace element characteristics of this potassic suite (depletions in Nb, low Zr/Ba and high K_2O/TiO_2 ratios) are considered diagnostic of a subduction-modified mantle source region (Hawkesworth and Vollmer 1979). However, subduction beneath North America west of central California ceased at ¥10–20 Ma due to the northward migration of the Mendocino triple junction (Atwater 1970). The Mono Basin area is currently part of the Basin and Range province, a region of block faulted mountain ranges and intervening basins that developed in response to approximately east-west extension that began at 13–10 Ma (Zoback et al. 1981). The potas-

sic suite of the Mono Basin region appears to have been erupted in an extensional environment that post-dates active subduction.

The East African Rift of Uganda

Phlogopite and biotite separates were obtained from several clinopyroxenite xenoliths that are abundant in the explosion craters of the Katwe-Kikorongo volcanic field in the western branch of the East African Rift and are found entrained in clinopyroxene-poor olivine melilitites and olivine-bearing nephelinites and leucitites. Detailed petrologic descriptions of the xenoliths have been presented elsewhere (Lloyd 1981, 1987; Lloyd et al. 1987) and only salient features are reported here. The typical mineralogy of the xenoliths is clinopyroxene + phlogopite/biotite + titanomagnetite + sphene + apatite. Two textural types can be identified in our group of samples: S23-209, -256, -262, -265 and parts of -268 have clinopyroxene and phlogopite or biotite forming an interlocking framework, which Davies and Lloyd (1986) identified as an original igneous texture. In contrast, phlogopite or biotite in samples S23-255, -267 and parts of -268 appear to be replacing clinopyroxene, suggesting a metasomatic origin (Lloyd 1981, 1987; Lloyd et al. 1987). Phase equilibrium experiments indicate that the nodules could represent either cognate cumulates or mantle xenoliths (Lloyd and Bailey 1975; Lloyd 1981; Arima and Edgar 1983; Lloyd et al. 1985). Chemical and isotopic differences between the host lavas and the nodule suite support a xenolith origin (Davies and Lloyd 1986). In addition, the overall style of trace element enrichment recorded by the Katwe-Kikorongo volcanism suggests an origin unrelated to subduction, and is more like that associated with ocean island volcanism (OIB; Davies and Lloyd 1986).

Ultrapotassic lamproites of the Leucite Hills, Wyoming

The ultrapotassic rocks of the Leucite Hills, Wyoming, consist of silica-undersaturated madupites and silica-saturated wyomingites and orendites, all of which are phlogopite-bearing lamproites. Phlogopite phenocrysts were separated from a wyomingite lava from North Table Mountain (sample LH-6: Carmichael 1967). The Leucite Hills volcanic field is considered Pleistocene on the basis of a single K-Ar date of 1.1 Ma for a phlogopite separate (MacDowell 1966). The lamproites erupted through Paleozoic-Eocene sediments (Malahoff and Moberly 1968), although the underlying basement is part of the Archean Wyoming craton. The trace element patterns of the Leucite Hills lavas are depleted in high field strength elements and enriched in the light rare earth and large ion lithophile elements, characteristics of subduction lavas (Kuehner et al. 1981; Vollmer et al. 1984) and unlike those of the Katwe-Kikorongo volcanic field. Moreover, the Nd and Sr isotope data indicate that enrichment of the Leucite Hills mantle source region probably occurred in the Archean (Vollmer et al. 1984).

Analytical techniques

Mineral separation

Clean phlogopite and biotite separates were obtained using organic heavy liquids and magnetic separation. Grains that contained inclusions, had rims or alteration along cleavage planes, or had any discoloration were then removed by hand-picking. The largest rims present in any of the mica grains prior to separation (based on back-scattered electron imaging) were <14 mm, representing $<0.01\%$ of the area of a grain in thin section, and any grains with rims were avoided during hand-picking. The largest grain size was used in order to sample phenocrysts preferentially rather than groundmass phlogopite in the lavas. For the lavas from Mexico, individual phlogopite phenocrysts exceeding 1 mm diameter were picked out from the crushed rock and subsequently crushed separately in acetone for hand-picking. Phlogopite and biotite grains in the xenoliths from Uganda are generally between 1–3 mm in diameter (Lloyd 1972); mesh sizes -30 to -60 or -60 to -90 were used for analysis.

Electron microprobe

Quantitative analyses were obtained on polished grain mounts of mineral separates and polished thin sections using the Cameca CAMEBAX electron microprobe at the University of Michigan. The microprobe was configured with four diffracting crystals (TAP, PET, LIF and OV60, the latter being for F and O analyses). A wide range of natural and synthetic standards were chosen in order to match as closely as possible the composition of the phase (Appendix). Standard operating conditions for mica analysis were an accelerating potential of 12 kV, a sample current of 10 nA and a 9 mm^2 rastered beam. A count time of 30 s was used for most elements, with 60 s for F and O. The potential for alkali and halogen loss was evaluated by conducting time-series experiments with the spectrometers centered on the peaks of interest and was determined not to occur within the time of a conventional quantitative analysis. Analytical data were corrected using the on-line Cameca PAP correction program. Analytical errors are given in Table 1. Standards were continually monitored during routine analysis in order to ensure accurate results. The FeO was measured by wet chemistry whereas total iron (FeO^T) was obtained by the electron microprobe. The wt% concentration of Fe_2O_3 was calculated as: wt% Fe_2O_3 = 1.1113*(wt% FeO^T - wt% FeO).

Wet chemistry

Colorimetric determination of wt% FeO was performed at the University of California, Berkeley, following the procedure described by Wilson (1960). Between 3 and 8 mg of sample as used. There was no photochemical reduction of ferric iron during the analyses, although this was evaluated (see Lange and Carmichael 1989 for a discussion). On the basis of repeat analyses of a glassy mid-ocean ridge basalt (JDFD-2), the precision of this method is $+0.21$ wt% FeO (2s). Replicate measurements of the mica separates were always within this precision.

Water and stable isotope analyses

The H_2O content and D/H ratio of phlogopite, biotite and hornblende separates were determined following the technique of Vennemann and O'Neil (1993). Samples were dried overnight at 100°C to remove adsorbed water. Between 30 and 70 mg of separate was loaded into silica-glass tubes along with 100 to 200 mg of coarse-grained quartz and a cap of quartz wool and heated under vacuum at 150°C for a minimum of two hours. The samples were then fused under vacuum to liberate all structural H as H_2O which was then separated cryogenically from any other gases released. Any molecular hydrogen produced during fusion was oxidized by CuO to H_2O and combined with the other water. All H_2O was collected in tubes containing Zn and reacted to form ZnO and H_2 gas. In addition to the isotopic analysis of this gas, the amount of water (in mg) was determined by measuring the intensity of mass-2 in a fixed volume (previously calibrated) on a Finnigan-MAT Delta-S mass spectrometer. One sigma precisions of this method are routinely better than $+0.1$ wt% H_2O and $+1$–2‰ dD. At the University of Michigan, the following analyses are obtained for the NBS-30 biotite standard: dD = -65‰ and wt% H_2O = 3.5. Oxygen isotope ratios were determined for three phlogopite separates (Mas-3a, -4 and -11). Oxygen was liberated from the minerals by reaction with ClF_3 at 550°C (Borthwick and Harmon 1982; Vennemann and Smith 1990) and converted to CO_2 for oxygen isotope analysis. All isotopic analyses are reported in the standard d notation relative to SMOW.

Results

Chemical compositions of phlogopite and biotite separates, including FeO, Fe_2O_3 and H_2O contents from electron microprobe, wet chemical and mass spectrometric analyses, are given in Table 1. The nomenclature adopted here is after Deer et al. (1962): phlogopite has mol% $Mg/Fe^T > 2:1$ and biotite has mol% $Mg/Fe^T < 2:1$. Analyses of various phenocryst phases coexisting with phlogopite or biotite have been made for several samples: olivine in three minette lavas (Mas-3a, -4, -11); clinopyroxene in a phlogopite-clinopyroxenite (B37-5) and in a minette lava (Mas-141); and hornblende in two andesite lavas (SN-31, SN-161). The average compositions of each of these phases are given in Table 1.

Shown in Table 2 are mica mineral formulae that were obtained by normalizing the data in Table 1 to 24 = O+OH+F+Cl (Deer et al. 1962). Because wt% H_2O and FeO contents are obtained from bulk samples, cation and anion contents from electron microprobe analyses were also averaged, including cores and rims. A large range in compositional zoning will translate into significant uncertainty in the calculated amount of Fe^{3+} and Fe^{2+} per formula unit (pfu)[1]. The maximum uncertainty in the calculated amount of Fe^{3+} pfu caused solely by zoning was estimated by assuming that all of the FeO^T zoning was caused by variations in Fe^{3+}. Combined errors from the microprobe and wet chemistry contribute an additional source of error. This total uncertainty in Fe^{3+} is 0.08–0.11 ions pfu for samples from western Mexico, 0.15–0.25 ions pfu for Mono Basin samples, 0.13 ions pfu for Leucite Hills and 0.10–0.16 ions pfu for the Uganda samples. These errors are smaller than the symbols used in Fig. 2.

Mineral chemistry

There is significant variation in the H_2O and Fe_2O_3 contents of the phlogopite and biotite samples both within and between the four sample localities. The Fe_2O_3 contents range from 0.8 to 10.5 wt%, corresponding to 0.09 to 1.15 Fe^{3+} pfu. Water contents vary from 1.6 to 3.0 wt%, corresponding to 1.58 to 3.04 OH pfu, significantly less than if an hydroxyl site were fully occupied (4.00 pfu). This deficiency is made up only in part by F and Cl and presumably is taken up by O substituting for OH.

The Fe^{3+}/Fe^T ratio obtained for the phlogopite separate from the Leucite Hills (23%) is far lower than that (73%) obtained by Cross (1897) for phlogopite of almost identical bulk composition, but from a different lava flow (Pilot Butte, Leucite Hills). This discrepancy in the Fe^{3+}/Fe^T ratio of the two phlogopite separates underscores the difficulty in interpreting some older data. Although the quality of Cross' wet chemical analysis is excellent, the wet chemical technique by which ferrous iron was measured prior to the 1940s was subject to atmospheric oxidation during boiling (Carmichael, personal communication). Moreover, there is currently no way to evaluate whether or not the mineral separate that Cross analyzed was completely unaffected by alteration.

The presence of low-temperature alteration minerals such as chlorite can significantly modify the mineral chemistry and the D/H ratios because of their relatively high H_2O (10–13 wt%) and negligible K_2O contents, and the large hydrogen isotope fractionation factor between water and chlorite (Marumo et al. 1980; Graham et al. 1987). No chlorite intergrowths were observed by backscattered electron imaging in any of the samples (Fig. 1) at a resolution of ¥0.2 mm (Goldstein et al. 1981). Four mica samples were also analyzed by powder X-ray diffractometry: Mas-3a, a low-dD western Mexico phlogopite (see stable isotope section, below), Mas-141, a high-dD western Mexico phlogopite; SN-31 from a Mono Basin andesite, and S23-267 from Uganda. None of the samples had the 7.07–7.21Å peak characteristic of chlorite group minerals within the limits of detection (<5%). Hence, chlorite does not contribute significantly to the bulk analyses of H_2O and FeO in our separates.

Biotite normalization schemes

The problems inherent in generating a mineral formula from microprobe data alone for hydrous species that contain both Fe^{2+} and Fe^{3+}, such as mica and amphibole, have long been recognized (Bohlen et al. 1980; Holdaway 1980; Dymek 1983; Hewitt and Abrecht 1986; Afifi and Essene 1988; Cosca et al. 1991; Dyar et al. 1991; Schumacher 1991). Afifi and Essene (1988) showed that cation and anion normalization schemes for biotite both generate formulae that are stoichiometric with good totals (adjusted for water contents) but nonetheless make incorrect estimates of the amounts of Fe_2O_3, FeO and H_2O. Anion normalization schemes for hornblendes made solely on the basis of electron microprobe data cannot replicate the measured Fe_2O_3 and H_2O, whereas fixed-cation normalization schemes provide a fair estimate of Fe_2O_3 but not H_2O contents (Cosca et al. 1991). Both types of schemes, however, are able to provide accurate mineral formulae for most other cations. Schumacher (1991) showed how errors in the mineral formula of biotite caused by incomplete chemical analyses propagate in geothermometry and geobarometry calculations.

One common method for obtaining mineral formulae of biotites from microprobe data alone is to normalize the sum of the atomic proportion of oxygen from each oxide to a charge of 44 (often designated as 22 oxygen equivalents), assuming all iron is Fe^{2+}. By normalizing biotites to a set charge, the number of cations obtained may be less than 16, resulting in apparent vacancies that are assigned to the interlayer (A) and/or octahedral sites.

[1] The use of per formula unit (pfu) here and throughout the text refers to mineral formulae that were obtained by normalizing the data, including FeO, Fe_2O_3 and H_2O to 24 = O+OH+F+Cl

Table 1 Analyses of phlogopite, biotite and coexisting phases, including measured FeO, Fe_2O_3, H_2O and dD values (*n*=number of probe analyses averaged; *b.d.*=below detection; *n.a.*=not analyzed or not applicable; *phl*=phlogopite; *bt*=biotite; *hbd*=hornblende; *ol*=olivine; *cpx*=clinopyroxene. Phlogopite $Mg/Fe^T > 2:1$; biotite $Mg/Fe^T < 2:1$)[a]

	Continental arc, western Mexico								Leucite Hills	East African Rift, Uganda	
Sample	Mas-3a	Mas-3a	Mas-4	Mas-4	Mas-11	Mas-11	Mas-141	Mas-141	LH-6	S23-209	S23-255
phase	phl n=12	ol n=37	phl n=16	ol n=15	phl n=16	ol n=35	phl n=8	cpx n=27	phl n=15	phl n=7	phl n=6
SiO_2	40.07	39.73	39.74	39.54	39.68	39.61	39.28	50.98	41.33	36.78	35.93
TiO_2	2.03	n.a.	2.47	n.a.	2.23	n.a.	2.93	1.09	2.12	4.44	5.65
Al_2O_3	13.41	0.01	13.96	0.02	13.82	0.03	14.08	2.39	12.10	14.24	14.46
Cr_2O_3	1.18	0.05	0.95	0.01	0.87	0.01	0.47	0.01	0.95	0.04	0.13
Fe_2O_3	3.70	n.a.	4.24	n.a.	4.68	n.a.	5.68	n.a.	0.81	5.21	4.18
FeO	0.82	n.a.	1.47	n.a.	0.62	n.a.	1.45	n.a.	2.48	9.41	9.03
FeO^T	n.a.	12.93	n.a.	11.76	n.a.	12.87	n.a.	6.51	n.a.	n.a.	n.a.
NiO	0.38	0.22	0.12	0.40	0.29	0.32	0.18	b.d.	0.23	0.11	b.d.
MnO	0.01	0.23	0.02	0.19	b.d.	0.24	0.07	0.18	0.03	0.08	0.10
MgO	23.36	45.74	22.61	47.12	23.37	46.08	21.85	15.11	24.94	16.25	16.29
BaO	0.59	n.a.	0.43	n.a.	0.40	n.a.	0.61	n.a.	0.43	0.59	b.d.
CaO	b.d.	0.21	0.09	0.16	0.01	0.21	b.d.	22.46	0.01	b.d.	0.01
Na_2O	0.50	n.a.	0.52	n.a.	0.60	n.a.	0.63	0.33	0.15	0.38	0.46
K_2O	10.38	n.a.	9.72	n.a.	10.22	n.a.	10.25	b.d.	10.90	9.74	10.02
F	1.29	n.a.	1.16	n.a.	1.23	n.a.	0.82	n.a.	1.44	0.03	0.24
Cl	0.01	n.a.	0.02	n.a.	0.02	n.a.	b.d.	n.a.	b.d.	0.01	b.d.
H_2O	2.14, 2.38	n.a.	2.33	n.a.	2.42	n.a.	2.39	n.a.	2.36	3.02, 3.04	2.41
O≡F	−0.54	n.a.	−0.49	n.a.	−0.52	n.a.	−0.35	n.a.	−0.60	−0.01	−0.10
O≡Cl	0.00	n.a.	−0.01	n.a.	0.00	n.a.	0.00	n.a.	0.00	0.00	0.00
Total	99.34	99.14	99.38	99.22	99.92	99.37	100.35	99.29	99.66	100.32	98.82
Fe^{3+}/Fe^T	0.802	n.a.	0.772	n.a.	0.872	n.a.	0.779	n.a.	0.227	0.333	0.294
dD_{SMOW}	−137, −103	n.a.	−129	n.a.	−56	n.a.	−43	n.a.	n.a.	−50, −60	−51

	East African rift, Uganda							Mono Basin, California			
Sample	S23-256	S23-262	S23-265	S23-267	S23-268	B37-5	B37-5	SN-31	SN-31	SN-161	SN-161
phase	phl n=8	bt n=8	bt n=13	bt n=8	bt n=8	phl n=12	cpx n=30	bt n=12	hbd n=20	phl n=19	hbd n=12
SiO_2	36.10	35.29	35.26	35.63	36.55	36.14	46.43	36.98	42.27	36.34	43.15
TiO_2	5.51	5.05	3.40	4.35	4.94	6.77	2.46	5.07	3.20	4.65	2.52
Al_2O_3	14.30	14.16	14.32	13.93	14.17	15.36	5.36	14.30	11.56	14.92	10.93
Cr_2O_3	0.01	0.11	0.01	0.19	0.12	b.d.	0.11	b.d.	0.05	0.01	0.01
Fe_2O_3	4.64	7.23	5.98	4.96	5.90	4.80	3.23	10.45	6.73	9.94	6.90
FeO	8.86	12.36	16.14	11.29	13.01	6.68	4.22	7.40	5.75	4.72	5.69
FeO^T	n.a.	n.a.	n.a.	n.a.	n.a.	n.a.	n.a.	n.a.	n.a.	n.a.	n.a.
NiO	0.03	0.02	b.d.	0.29	0.02	0.06	0.01	0.05	b.d.	0.08	b.d.
MnO	0.08	0.22	0.32	0.38	0.22	0.15	0.08	0.16	0.18	0.13	0.21
MgO	15.91	12.46	11.26	14.54	12.23	16.59	12.04	14.33	13.53	15.80	13.83
BaO	b.d.	0.18	0.34	0.12	0.04	1.06	n.a.	1.19	n.a.	1.32	n.a.
CaO	0.08	b.d.	b.d.	0.09	0.02	0.03	23.60	0.04	11.34	0.07	11.35
Na_2O	0.34	0.40	0.37	0.51	0.34	0.49	0.62	0.80	2.21	0.93	2.19
K_2O	9.87	9.86	9.69	9.49	9.79	9.64	n.a.	8.94	1.08	8.41	0.93
F	0.00	0.13	b.d.	1.09	b.d.	0.14	n.a.	0.15	0.12	0.06	0.10
Cl	0.02	b.d.	0.01	0.04	0.01	0.02	n.a.	0.05	0.03	0.04	0.02
H_2O	2.92	2.41	2.97	2.63	2.34	2.17	n.a.	1.57	0.91	2.41	1.23
O≡F	0.00	−0.06	0.00	−0.46	0.00	−0.06	n.a.	−0.07	−0.05	−0.03	−0.04
O≡Cl	0.00	0.00	0.00	−0.01	0.00	0.00	n.a.	−0.01	−0.01	−0.01	0.00
Total	98.66	99.82	100.07	99.07	99.70	100.04	98.17	101.40	99.57	99.78	99.02
Fe^{3+}/Fe^T	0.320	0.345	0.250	0.265	0.290	0.393	n.a.	0.560	n.a.	0.654	n.a.
dD_{SMOW}	−49	−50	−70	−58	−57	−59	n.a.	−53	−53	n.a.	−65

[a] Maximum relative error (2s), for phlogopite and biotite analyses, based on counting statistics on the electron microprobe: Si 0.01; Ti 0.11; Al 0.01; Cr 0.61; Fe^T 0.05; Ni 0.32; Mn 0.44; Mg 0.01; Ba 0.74; Ca 0.29; Na 0.16; K 0.02; F 0.08; Cl 0.55. FeO from wet chemistry and Fe_2O_3 determined by difference: Fe_2O_3 wt%=1.1113 (FeO^T-FeO) wt%. H_2O and dD_{SMOW} determined by mass spectrometry

Table 2 Calculated mineral formulae. See footnote on page 58 for methods A, B and C

Sample	Mexico: Mas-3a			Mexico: Mas-4			Mexico: Mas-11			Mexico: Mas-141			Leucite Hills			Uganda: S23-209		
Method[a]	A	B	C	A	B	C	A	B	C	A	B	C	A	B	C	A	B	C
Wt%																		
Fe_2O_3	3.70	0.00	0.00	4.24	0.00	0.00	4.68	0.00	0.00	5.68	0.00	0.00	0.81	0.00	0.00	5.21	0.00	0.00
FeO	0.82	4.15	4.15	1.47	5.29	5.29	0.62	4.82	4.82	1.45	6.55	6.55	2.48	3.20	3.20	9.41	14.10	14.10
H_2O	2.14	2.95	3.59	2.33	3.08	3.65	2.42	3.15	3.63	2.39	3.11	3.81	2.36	3.00	3.56	3.03	3.32	4.03
Total	99.34	99.77	100.42	99.38	99.70	100.27	99.92	100.17	100.66	100.35	100.49	101.20	99.66	100.21	100.78	100.32	100.08	100.80
# ions																		
Si	5.834	5.791	5.715	5.765	5.734	5.669	5.725	5.704	5.648	5.697	5.689	5.609	5.970	5.907	5.839	5.498	5.533	5.452
Al_{iv}	2.166	2.209	2.254	2.235	2.266	2.331	2.275	2.296	2.319	2.303	2.311	2.369	2.030	2.038	2.015	2.502	2.467	2.487
Fe^{3+}_{iv}	0.000	0.000	0.000	0.000	0.000	0.000	0.000	0.000	0.000	0.000	0.000	0.000	0.000	0.000	0.000	0.000	0.000	0.000
Ti_{iv}	0.000	0.000	0.031	0.000	0.000	0.000	0.000	0.000	0.033	0.000	0.000	0.022	0.000	0.055	0.146	0.000	0.000	0.062
Al_{vi}	0.136	0.075	0.000	0.151	0.109	0.016	0.075	0.045	0.000	0.103	0.092	0.000	0.029	0.000	0.000	0.006	0.057	0.000
Ti_{vi}	0.222	0.220	0.187	0.269	0.268	0.265	0.242	0.241	0.205	0.320	0.319	0.293	0.230	0.172	0.079	0.499	0.502	0.433
Cr	0.136	0.135	0.134	0.109	0.109	0.108	0.099	0.099	0.098	0.053	0.053	0.053	0.108	0.107	0.106	0.005	0.005	0.005
Fe^{3+}	0.406	0.000	0.000	0.463	0.000	0.000.	0.508	0.000	0.000	0.619	0.000	0.000	0.088	0.000	0.000	0.587	0.000	0.000
Fe^{2+}	0.100	0.501	0.495	0.178	0.638	0.631	0.075	0.580	0.574	0.176	0.794	0.782	0.300	0.383	0.379	1.176	1.774	1.748
Ni	0.045	0.035	0.044	0.014	0.011	0.014	0.033	0.026	0.033	0.021	0.017	0.021	0.026	0.020	0.026	0.013	0.010	0.013
Mn	0.001	0.001	0.001	0.003	0.003	0.003	b.d.	b.d.	b.d.	0.008	0.008	0.008	0.004	0.004	0.004	0.010	0.010	0.010
Mg	5.071	5.032	4.968	4.889	4.863	4.808	5.028	5.008	4.960	4.725	4.717	4.652	5.371	5.313	5.254	3.620	3.642	3.589
vi site	6.116	6.000	5.827	6.078	6.000	5.844	6.060	6.000	5.871	6.026	6.000	5.809	6.156	6.055	5.847	5.916	6.000	5.798
Ba	0.034	0.033	0.033	0.024	0.024	0.024	0.022	0.022	0.022	0.035	0.035	0.034	0.024	0.024	0.024	0.034	0.035	0.034
Ca	b.d.	b.d.	b.d.	0.014	0.014	0.014	0.001	0.001	0.001	b.d.	b.d.	b.d.	0.001	0.001	0.001	b.d.	b.d.	b.d
Na	0.140	0.139	0.137	0.147	0.146	0.145	0.168	0.167	0.165	0.179	0.178	0.176	0.042	0.041	0.041	0.109	0.110	0.108
K	1.929	1.914	1.889	1.798	1.789	1.769	1.881	1.874	1.856	1.896	1.894	1.867	2.009	1.988	1.966	1.857	1.869	1.842
A site	2.103	2.087	2.060	1.984	1.973	1.951	2.072	2.065	2.045	2.110	2.107	2.077	2.077	2.054	2.031	2.001	2.014	1.984
O	20.000	20.000	20.000	20.000	20.000	20.000	20.000	20.000	20.000	20.000	20.000	20.000	20.000	20.000	20.000	20.000	20.000	20.000
O	1.326	0.562	0.000	1.206	0.499	0.000	1.106	0.418	0.000	1.309	0.614	0.000	1.069	0.493	0.000	0.961	0.648	0.000
F	0.593	0.588	0.581	0.534	0.531	0.525	0.561	0.558	0.553	0.377	0.377	0.372	0.656	0.649	0.642	0.015	0.015	0.015
Cl	0.003	0.003	0.003	0.006	0.006	0.006	0.004	0.004	0.004	b.d.	b.d	b.d.	0.001	0.001	0.001	0.003	0.003	0.003
OH	2.078	2.846	3.416	2.254	2.964	3.469	2.329	3.019	3.443	2.312	3.008	3.627	2.274	2.857	3.357	3.021	3.334	3.982

Table 2 (continued)

Sample	Uganda: S23-255			Uganda: S23-256			Uganda: S23-262			Uganda: S23-265			Uganda: S23-267			Uganda: S23-268		
Method	A	B	C	A	B	C	A	B	C	A	B	C	A	B	C	A	B	C
Wt%																		
Fe_2O_3	4.18	0.00	0.00	4.64	0.00	0.00	7.23	0.00	0.00	5.98	0.00	0.00	4.96	0.00	0.00	5.90	0.00	0.00
FeO	9.03	12.79	12.79	8.86	13.04	13.04	12.36	18.87	18.87	16.14	21.52	21.52	11.29	15.76	15.76	13.01	18.31	18.31
H_2O	2.41	3.00	3.92	2.92	3.05	4.01	2.41	3.04	3.88	2.97	3.34	3.89	2.63	2.77	3.42	2.34	2.87	3.98
Total	98.82	98.98	99.91	98.66	98.52	99.28	99.82	99.72	100.56	100.07	99.84	100.39	99.07	98.68	99.37	99.70	99.64	100.75
# ions																		
Si	5.458	5.446	5.342	5.460	5.506	5.396	5.442	5.464	5.367	5.465	5.501	5.437	5.441	5.492	5.414	5.619	5.635	5.504
Al_{iv}	2.542	2.554	2.533	2.540	2.494	2.519	2.558	2.536	2.539	2.535	2.499	2.563	2.507	2.508	2.495	2.381	2.365	2.496
Fe^{3+}_{iv}	0.000	0.000	0.000	0.000	0.000	0.000	0.000	0.000	0.000	0.000	0.000	0.000	0.052	0.000	0.000	0.000	0.000	0.000
Ti_{iv}	0.000	0.000	0.125	0.000	0.000	0.085	0.000	0.000	0.094	0.000	0.000	0.000	0.000	0.000	0.091	0.000	0.000	0.000
Al_{vi}	0.047	0.028	0.000	0.008	0.076	0.534	0.017	0.049	0.000	0.081	0.134	0.039	0.000	0.023	0.000	0.186	0.210	0.019
Ti_{vi}	0.646	0.644	0.458	0.626	0.632	0.619	0.586	0.589	0.484	0.396	0.399	0.394	0.500	0.505	0.407	0.571	0.573	0.560
Cr	0.016	0.016	0.016	0.001	0.001	0.001	0.013	0.013	0.013	0.001	0.001	0.001	0.023	0.024	0.023	0.015	0.015	0.015
Fe^{3+}	0.477	0.000	0.000	0.528	0.000	0.000	0.840	0.000	0.000	0.697	0.000	0.000	0.519	0.000	0.000	0.682	0.000	0.000
Fe^{2+}	1.147	1.620	1.590	1.121	1.663	1.630	1.594	2.443	2.400	2.092	2.807	2.774	1.442	2.031	2.002	1.672	2.361	2.306
Ni	b.d.	b.d.	b.d.	0.004	0.003	0.003	0.002	0.002	0.002	b.d.	b.d.	b.d.	0.036	0.029	0.036	0.003	0.002	0.003
Mn	0.013	0.013	0.012	0.010	0.010	0.010	0.029	0.029	0.028	0.041	0.042	0.041	0.049	0.049	0.048	0.028	0.028	0.028
Mg	3.688	3.679	3.609	3.586	3.616	3.545	2.864	2.875	2.824	2.601	2.617	2.587	3.310	3.340	3.294	2.803	2.811	2.746
vi site	6.034	6.000	5.733	5.885	6.000	5.722	5.945	6.000	5.753	5.910	6.000	5.838	5.879	6.000	5.811	5.961	6.000	5.676
Ba	b.d.	b.d.	b.d.	b.d.	b.d.	b.d.	0.011	0.011	0.011	0.021	0.021	0.021	0.007	0.007	0.007	0.003	0.003	0.003
Ca	0.002	0.002	0.002	0.012	0.012	0.012	b.d.	b.d.	b.d.	b.d.	b.d.	b.d.	0.015	0.015	0.015	0.003	0.003	0.003
Na	0.136	0.136	0.133	0.100	0.101	0.099	0.119	0.119	0.117	0.112	0.113	0.111	0.152	0.153	0.151	0.102	0.103	0.100
K	1.943	1.938	1.901	1.905	1.921	1.883	1.939	1.947	1.912	1.915	1.928	1.905	1.849	1.867	1.840	1.919	1.924	1.880
A site	2.081	2.076	2.036	2.017	2.034	1.994	2.069	2.077	2.040	2.048	2.061	2.038	2.024	2.042	2.014	2.027	2.032	1.985
O	20.000	20.000	20.000	20.000	20.000	20.000	20.000	20.000	20.000	20.000	20.000	20.000	20.000	20.000	20.000	20.000	20.000	20.000
O	1.440	0.855	0.000	1.049	0.891	0.000	1.455	0.791	0.000	0.926	0.516	0.000	0.786	0.612	0.000	1.599	1.043	0.000
F	0.117	0.117	0.115	b.d.	b.d.	b.d.	0.065	0.066	0.065	b.d.	b.d.	b.d.	0.526	0.530	0.523	b.d.	b.d.	b.d.
Cl	b.d.	b.d.	b.d.	0.005	0.006	0.005	b.d.	b.d.	b.d.	0.003	0.003	0.003	0.009	0.009	0.009	0.002	0.002	0.002
OH	2.442	3.028	3.885	2.945	3.103	3.995	2.479	3.143	3.935	3.070	3.480	3.997	2.679	2.848	3.468	2.399	2.955	3.998

(*Continued*)

Table 2 (continued)

Sample	Uganda: B37-5			Mono Basin: SN-31			Mono Basin: SN-161		
Method	A	B	C	A	B	C	A	B	C
Wt%									
Fe_2O_3	4.80	0.00	0.00	10.45	0.00	0.00	9.94	0.00	0.00
FeO	6.68	11.00	11.00	7.40	16.80	16.80	4.72	13.66	13.66
H_2O	2.17	2.74	4.04	1.57	3.03	3.99	2.41	3.15	4.00
Total	100.04	99.98	101.43	101.40	101.79	102.77	99.78	99.51	100.38
# ions									
Si	5.418	5.415	5.272	5.586	5.554	5.444	5.452	5.497	5.399
Al_{iv}	2.582	2.585	2.641	2.414	2.446	2.481	2.548	2.503	2.601
Fe^{3+}_{iv}	0.000	0.000	0.000	0.000	0.000	0.000	0.000	0.000	0.000
Ti_{iv}	0.000	0.000	0.087	0.000	0.000	0.075	0.000	0.000	0.000
Al_{vi}	0.131	0.127	0.000	0.131	0.085	0.000	0.090	0.156	0.012
Ti_{vi}	0.764	0.763	0.656	0.576	0.573	0.486	0.524	0.528	0.519
Cr	b.d.	b.d.	b.d.	b.d.	b.d.	b.d.	0.002	0.002	0.002
Fe^{3+}	0.542	0.000	0.000	1.188	0.000	0.000	1.122	0.000	0.000
Fe^{2+}	0.837	1.378	1.342	0.934	2.110	2.069	0.592	1.728	1.697
Ni	0.007	0.005	0.007	0.006	0.005	0.006	0.010	0.008	0.010
Mn	0.019	0.019	0.019	0.020	0.020	0.019	0.016	0.016	0.016
Mg	3.709	3.706	3.609	3.227	3.208	3.145	3.534	3.562	3.500
vi site	6.010	6.000	5.633	6.083	6.000	5.726	5.890	6.000	5.756
Ba	0.062	0.062	0.060	0.070	0.070	0.069	0.077	0.078	0.077
Ca	0.004	0.004	0.004	0.006	0.006	0.006	0.012	0.012	0.012
Na	0.143	0.143	0.139	0.235	0.234	0.229	0.269	0.271	0.267
K	1.844	1.843	1.794	1.722	1.712	1.679	1.609	1.622	1.594
A site	2.053	2.052	1.998	2.033	2.022	1.982	1.968	1.983	1.949
O	20.000	20.000	20.000	20.000	20.000	20.000	20.000	20.000	20.000
O	1.759	1.187	0.000	2.332	0.881	0.000	1.550	0.784	0.000
F	0.067	0.066	0.065	0.074	0.073	0.072	0.029	0.029	0.028
Cl	0.005	0.005	0.005	0.012	0.012	0.012	0.010	0.010	0.010
OH	2.170	2.742	3.931	1.582	3.033	3.916	2.412	3.177	3.962

Normalization procedure: **A** calculated by normalizing around 24=O+OH+F+Cl with measured FeO, Fe_2O_3, and H_2O; **B** calculated by normalizing around 14 cations, with measured total iron only; **C** calculated by normalizing around 44 anions, with measured total iron only. Tetrahedral site preference of $Si>Al>Fe^{3+}>Ti$

The amount of H_2O is calculated by assuming OH = 4−(F+Cl). Once the analyses are normalized to a given anionic charge, there is no unique method for estimating the Fe_2O_3/FeO ratio (Cosca et al. 1991; Schumacher 1991). A second method for recalculating microprobe analyses is to normalize on the basis of a given number of cations. For trioctahedral micas, a fixed number of octahedral and tetrahedral cations is used (14 = Si+Ti+Al+Fe+Mn+Mg+Sr+Ni). Any excess negative charge is compensated by replacing Fe^{2+} with Fe^{3+}, whereas excess positive charge is compensated by replacing OH with excess oxygen, thus giving a minimum estimate of ferric iron. The amount of H_2O is calculated by OH = 24−(O+F+Cl). The fixed-cation normalization method assumes that the octahedral site is fully occupied, although it does permit vacancies on the interlayer site. The presence of octahedral vacancies causes an overestimation of the mole fraction of each of the tetrahedral and octahedral cations in proportion to the number of vacancies, resulting in an excess positive charge (Dymek 1983).

To test the validity of these normalization schemes in biotite and phlogopite, calculated mineral formulae may be compared to those obtained by normalizing on the basis of 24 = O+OH+F+Cl using the results from wet chemical and mass spectrometric analyses of FeO, Fe_2O_3 and H_2O. In this procedure, it is assumed that the hydroxyl site is fully occupied, since vacancies are not stable in a closest packed site. For many cations, including Ti, Mg, Mn, Ca, Ba, Na as well as F and Cl, both the cation and anion normalization schemes provide fairly accurate mineral formulae (Table 2, Fig. 2). Both schemes provide less accurate estimates for Si, Al^T (total Al) and K. The normalization neglects the possibility of significant anion vacancies as did Foster (1960) and Deer et al. (1962). The most significant error is the overestimation of the amount of Fe^{2+} at the expense of Fe^{3+}, and the overestimation of OH at the expense of O on the hydroxyl site. For all of the samples analyzed here, the fixed-cation normalization procedure results in an excess positive charge that is compensated by the replacement of OH by O in order to charge balance the mineral formulae. This compensation is reflected in the apparent increase in accuracy of OH by the fixed-cation normalization procedure compared to the anionic charge method, whereas the amount of Fe^{2+} and Fe^{3+} remain equally inaccurate for both methods. These inaccuracies persist even though the adjusted totals (including calculated water contents) for the anion and cation normalization schemes are acceptable and calculated site occupancies appear to be stoichiometric. Thus, a good or bad total or the appearance of stoichiometry based on recalculated probe data alone is not a sufficient indicator of a good analysis, nor is this method useful for assessing the Fe^{3+}/Fe^{2+} or OH concentration in biotite.

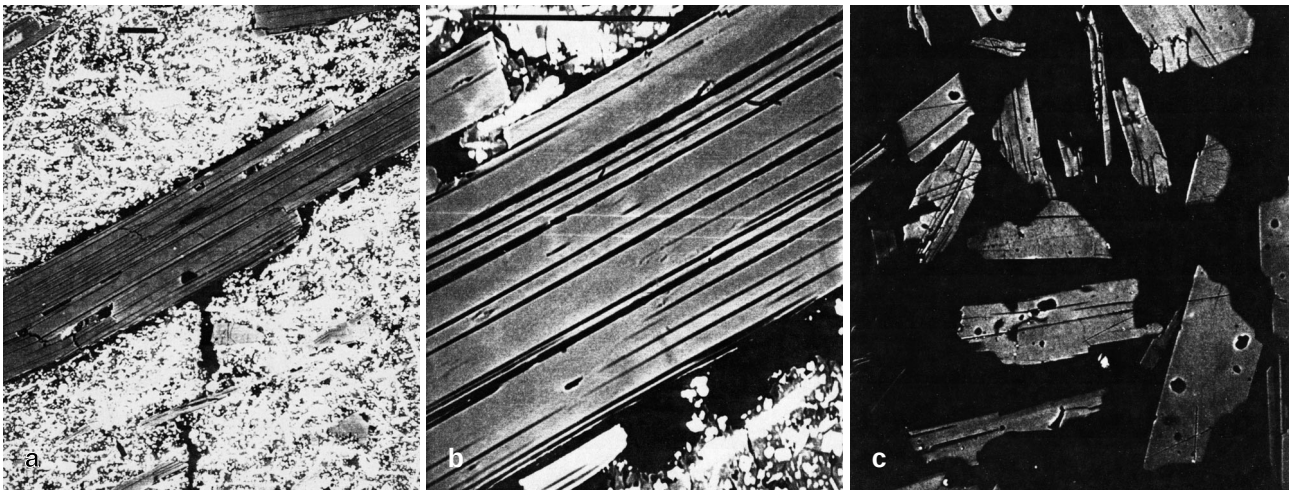

Fig. 1 **a** Backscattered electron (BSE) image of a phlogopite phenocryst from sample Mas-3a, a minette lava from western Mexico, magnified 80x. Scale bar = 100 mm. **b** Same as Fig. 1a, magnified 400x. Reaction rim on phenocrysts is <2 mm. Scale bar = 100 mm. **c** BSE image of phlogopite grain mounts for sample S23-268 from the East African Rift, Uganda, magnified 120x. Some grains contain small Fe-Ti oxide inclusions that were separated out during hand-picking and were not included in the separates used for FeO or water analyses

Electron microprobe determination of oxygen

The introduction of layered synthetic dispersion element (LSDE) crystals, such as the pseudo-crystal OV60, have increased the analytical capacity of the electron microprobe to include light elements such as oxygen (Armstrong 1988; Bastin and Heijligers 1989). In minerals like biotite and hornblende that contain both water *and* an element in two oxidation states, there is no unique way to determine both H_2O contents and Fe^{3+}/Fe^{2+} ratios even with direct measurement of oxygen. If, however, either H_2O or FeO has been measured directly, then a value for oxygen can be used to infer the concentration of the other. Several factors complicate the determination of oxygen on the microprobe, including variations in peak shape, absorption of oxygen by the carbon coating, contamination by surface water, large mass absorption coefficients and atomic number corrections (Armstrong 1988; Bastin and Heijligers 1989; Goldstein et al. 1991).

Oxygen contents were obtained in this study as part of electron microprobe analyses, using a hornblende megacryst from Kakanui, New Zealand (18.29 Si, 7.89 Al, 8.49 Fe, 7.72 Mg, 7.36 Ca, 1.93 Na, 1.70 K, 2.62 Ti, 42.91 O wt%) as the standard. Wavelength scans for this standard and fluorophlogopite, with the *c*-axis oriented parallel and perpendicular to the electron beam, indicate that peak shape and position for oxygen is nearly identical for all[2]. In Fig. 3, oxygen contents as determined on the electron microprobe and corrected using the Cameca PAP program are compared to oxygen contents obtained from the complete analysis of biotite [analytical total - (sum of cations + F + Cl)]. Absolute errors for the direct analysis of oxygen on the microprobe are 2s = 0.39 based on counting statistics, equivalent to those for the

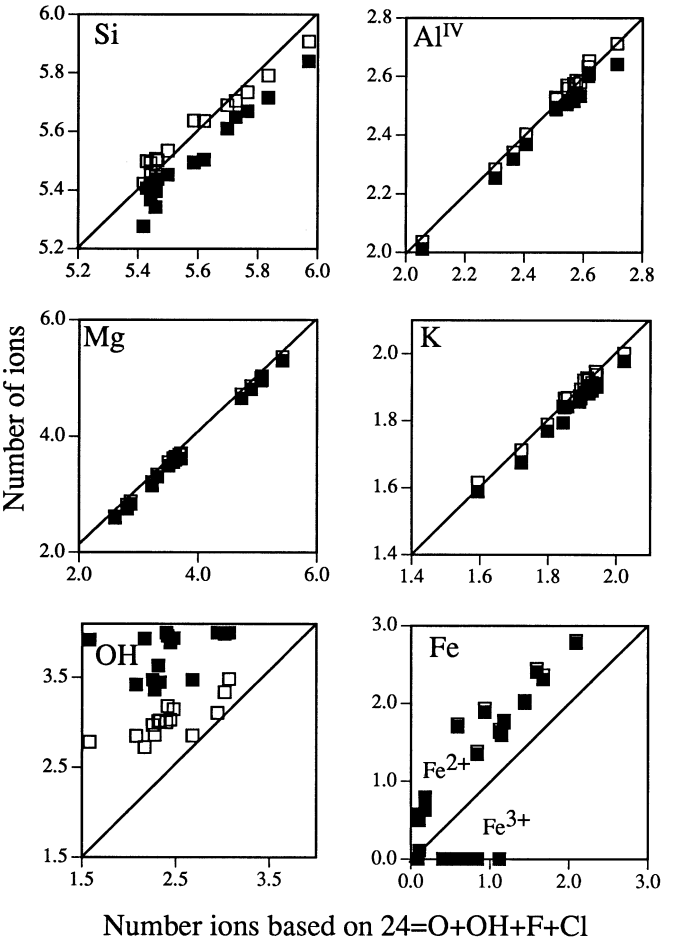

Fig. 2 Calculated number of ions per formula unit (pfu) based on 24 = O+OH+F+Cl with measured FeO, Fe_2O_3 and H_2O contents, versus calculated number of ions by normalizing to 14 cations (*open symbols*) or 44 anionic charge (*closed symbo*ls). The 1:1 correspondence line is shown. Normalization schemes are described in the text

[2] Details of oxygen analysis, including peak shapes, can be found in S.N. Feldstein (1997)

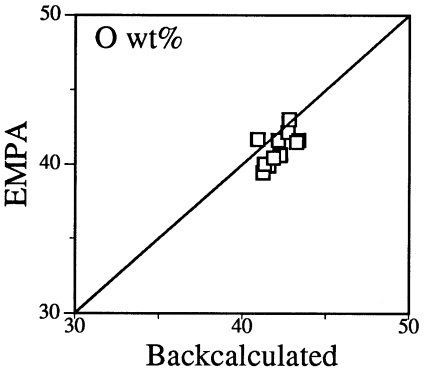

Fig. 3 Backcalculated oxygen wt% based on 24 = O+OH+F+Cl with measured FeO, Fe_2O_3 and H_2O contents, versus oxygen wt% measured directly on the electron microprobe (EMPA). The 1:1 correspondence line is shown

calculated oxygen contents and encompassed by the symbols in Fig. 3. Measured oxygen contents are low by ¥1.5% absolute. This discrepancy might be caused by variations in the thickness of the carbon coating between sample and standard (Goldstein et al. 1991).

Stable isotope analyses

The dD values of biotite and phlogopite analyzed in this study (Table 1; Fig. 4a) encompass a large range (−137 to −43‰). For comparison, the range in dD values of micas from other mafic magmatic rocks, including kimberlites, carbonatites and xenoliths in alkali basalts, fall between −95 and −25‰ (Sheppard and Epstein 1970; Kuroda et al. 1975, 1977; Sheppard and Dawson 1975; Boettcher and O'Neil 1980; Kyser and O'Neil 1984; Poreda 1985; Dobson and O'Neil 1987; Kyser and Stern 1988; Guy et al. 1992). Unaltered mid-ocean ridge basaltic glasses have dD values between −85 and −75‰, whereas back-arc basaltic glasses and primary cumulate hornblende from subduction-related lavas have dD values between −45 and −28 ‰ (Craig and Lupton 1976; Satake and Matsuda 1979; Kyser and O'Neil 1984; Guy et al. 1992). The phlogopite phenocrysts from western Mexico have the widest range in D/H ratio ever measured for minerals from arc lavas. Two aliquots of sample Mas-3a had different dD values as well as water contents (2.14 wt% H_2O, −137‰; 2.38 wt% H_2O, −103‰), indicating significant isotopic heterogeneity in this sample. Sample Mas-3a erupted alongside sample Mas-11 but over 400 thousand years later; the two lavas have almost identical major element whole rock and phlogopite compositions (including ferric-ferrous ratios and water contents) but remarkably different dD values of −137 and −56‰, respectively. Phlogopite phenocrysts from two other western Mexico lava flows had dD values of −129 and −43‰. Three minette lavas (Mas 3a, 4 and 11) with phlogopite phenocryst dD values of −137, −129 and −56‰, respectively, have $d^{18}O$ values of 5.2, 5.2 and 6.2‰ respectively.

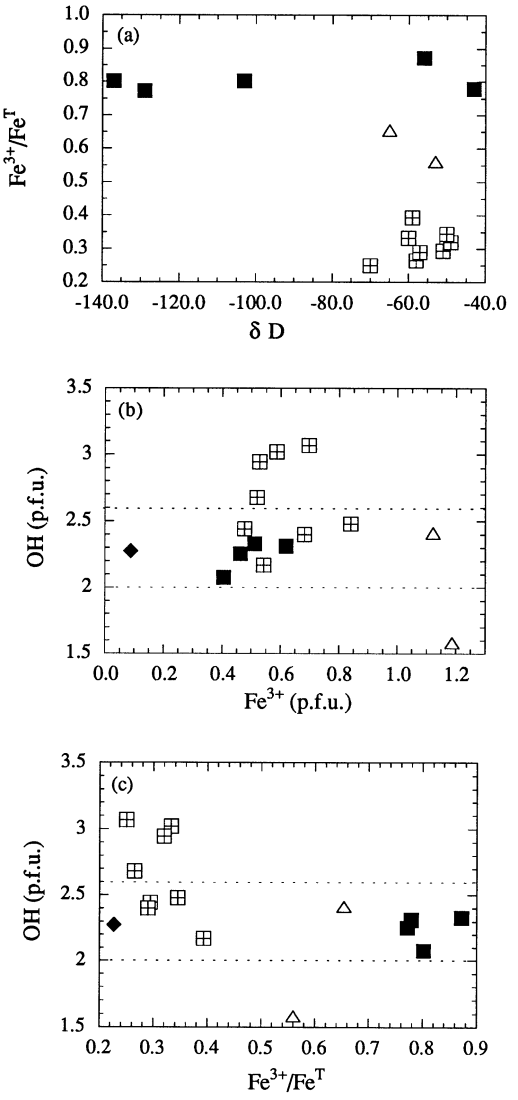

Fig. 4 **a** A plot of Fe^{3+}/Fe^T ratios vs dD for the micas analyzed in this study. *Solid squares* (western Mexico), *open triangles* (eastern California), *solid diamond* (Leucite Hills, Wyoming), *open squares enclosing a plus sign* (East African Rift, Uganda). **b** A plot of OH (per formula unit) vs Fe^{3+} (per formula unit) for the micas analyzed in this study; symbols as in **a**. **c** A plot of OH (per formula unit) vs Fe^{3+}/Fe^T for the micas analyzed in this study; symbols as in **a**

Biotite and hornblende phenocrysts from a single andesite sample from the Mono Basin area (SN-31) had identical dD values of −53‰; hornblende phenocrysts from a second andesite sample (SN-161) had a dD value of −65‰. (There is no dD value for SN-161 biotite because of an experimental failure.) The dD values of biotite and phlogopite from the Ugandan clinopyroxenites range from −70 to −49‰. Two aliquots of the phlogopite separate S23-209 had somewhat different dD values (−50 versus −60 ‰) with identical H_2O contents. This difference is well outside the analytical error (1–2‰) and such differences were not observed for standards analyzed at the same time. This observation suggests that some of the samples are isotopically heterogeneous.

There is no systematic difference in dD values between the two textural types identified in the Uganda xenoliths, one believed to be igneous and the other metasomatic in origin.

Discussion

Effect of magmatic degassing and post-eruptive oxidation on mineral chemistry

Before analyses of biotite phenocrysts can be used to infer pre-eruptive magmatic conditions, it must first be established that these analyses represent pristine minerals that have not been affected by a variety of alteration processes. For example, if magma is transported from deep crustal levels to a shallow reservoir where the pressure is sufficiently low that the magma becomes vapor-saturated, extensive degassing can occur prior to eruption. Hydrous phenocrysts, such as mica and hornblende, may partially dehydrate in response to a drop in water fugacity. Numerous disequilibrium experiments at 1 bar on biotite powders and flakes indicate that at high temperatures, dehydration can occur by dehydroxylation:

$$2OH^- \text{ V } O^{2-} + H_2O \quad (1)$$

(e.g., Vedder and Wilkins 1969; Sanz et al. 1983; Tikhomirova et al. 1989). This reaction generates a vacancy in the hydroxyl site, unstable in a closest packed site, and therefore leads to the breakdown of biotite and the development of reaction rims. Experiments by Rutherford and Hill (1993) on a dacite magma indicate that at least four days are required for the development of reaction rims on hornblende phenocrysts after a drop in water fugacity has occurred. The effect of Reaction 1 on reducing the measured hydroxyl concentration of the mica and hornblende phenocrysts relative to their pristine, magmatic values was minimized by hand-picking grains that were completely free of alteration rims.

In addition to Reaction 1, another dehydration mechanism can occur that affects the ferric-ferrous ratio in the mica. It is the oxidation/dehydrogenation reaction:

$$Fe^{2+} + OH^- \text{ V } Fe^{3+} + O^{2-} + \frac{1}{2} H_2 \quad (2)$$

(e.g., Sanz et al. 1983; Guttler et al. 1989; Rancourt et al. 1993). Unlike the case for Reaction 1, Reaction 2 is reversible and need not create opaque reaction rims on the mica and hornblende phenocrysts. Numerous experimental studies demonstrate that complete iron oxidation and dehydrogenation occurs in biotites when heated in air to 300–800°C (Hogg and Meads 1975; Ferrow 1987; Chandra and Lokanathan 1982, Sanz et al. 1983). However, in an inert atmosphere and in vacuum, complete oxidation is not achieved up to 800–1000°C (Rimsaite 1970; Chandra and Lokanathan 1982) and, in a reducing atmosphere, there is *no* oxidation of iron up to 1600°C (Chandra and Lokanathan 1982). The experimental evidence suggests that Reaction 2 will only proceed in hydrous phenocrysts if the host magma becomes oxidized, or if there is a drop in the fugacity of H_2.

A commonly invoked mechanism for the oxidation of magmatic liquids is the preferential loss of the H_2 or CO component through degassing (Sato 1978; Mathez 1984). Since both of these components have extremely low solubilities in magmatic liquids at oxygen fugacities $\geq$QFM (Dixon et al. 1991; Thibault and Holloway 1994), they are formed in the gas bubble only after the H_2O or CO_2 component has diffused from the melt to the gas, in which case no net oxidation of the melt has occurred. This argument is supported by a detailed study of gases collected from the Puu Oo eruption at Kilauea Volcano, Hawaii. Gerlach (1993) showed that all gases collected over a temperature interval of 1185 to 935°C had oxygen fugacities with a constant DNNO value of $-0.51 + 0.04$. This value is consistent with that calculated for Kilauean lavas based on Fe-Ti oxides and bulk ferric-ferrous ratios in the glassy lavas (Gerlach 1993). The evidence from Hawaii demonstrates that equilibrium degassing does not lead to oxidation or reduction of the residual magma.

Because Reaction 2 can only occur when there is a drop in the hydrogen fugacity of the system, the best opportunity for this to occur is during eruption into air. However, the Fe^{3+}/Fe^T ratios (80, 87 and 78%) in Mascota phlogopite phenocrysts found in slowly cooled lavas (Mas-3, -11, -141, respectively) are not significantly higher than the Fe^{3+}/Fe^T ratio (77%) found in phlogopite from a rapidly quenched scoria (Mas-4). Moreover, if Reaction 2 was an important process during eruption of the minette magmas into air, then all mica-bearing lavas should have mica phenocrysts that record similarly high Fe^{3+}/Fe^T ratios as those from western Mexico, which is clearly not the case. Lavas from eastern California and Wyoming that were examined in this study had micas with significantly lower Fe^{3+}/Fe^T ratios than those from western Mexico despite similar eruption histories. Therefore, the field evidence argues strongly against the importance of Reaction 2 during eruption into air. This is consistent with the lack of any correlation between Fe^{3+} (pfu) and OH (pfu) for the micas analyzed in this study (Fig. 4b).

Variation in Fe^{3+}/Fe^T with tectonic setting

The Fe^{3+}/Fe^T ratios and hydroxyl contents of the phlogopite and biotite samples in this study provide a qualitative measure of pre-eruptive f_{O_2} and f_{H_2O} in the magma. Although such an analysis is not quantitative without access to an activity-composition model for mica solid solutions, broad differences between tectonic settings may be assessed. The ratio of ferric iron to total iron for the separates analyzed in this study ranges from 23 to 87%, with phlogopite and biotite from different tectonic associations having characteristic Fe^{3+}/Fe^T ratios (Fig 4c). Ratios approaching 80–90% are possible because in addition to the oxyannite component, $KFe^{2+}Fe_2^{3+}AlSi_3O_{12}$,

which has a Fe^{3+}/Fe^{T} ratio of 66%, other components such as $KMgFe^{3+}_2AlSi_3O_{12}$ may also be present, with a Fe^{3+}/Fe^{T} ratio of 100%.

The phlogopite phenocrysts in minette lavas from the continental arc of western Mexico have the highest Fe^{3+}/Fe^{T} ratios of 77–87%, consistent with the high magmatic oxygen fugacities inferred for these lavas (3–5 log units above the Ni-NiO buffer; Lange and Carmichael 1991; Carmichael et al. 1996). Detailed petrologic and geochemical studies of the western Mexican arc lavas indicate that they have a geochemical signature characteristic of a subduction environment (Luhr et al. 1989; Lange and Carmichael 1991). Biotite phenocrysts from the Mono Basin andesite lavas, whose chemistry also is characteristic of a subduction environment (Lange et al. 1993) also have high Fe^{3+}/Fe^{T} of 56–66%. The oxygen fugacities of these lavas are between 1–2 log units above Ni-NiO (Lange and Carmichael 1996).

In contrast to the high Fe^{3+}/Fe^{T} ratios found in micas from arc lavas, biotite and phlogopite separates from Uganda clinopyroxenite xenoliths have lower Fe^{3+}/Fe^{T} ratios (25–40%). These low ratios relative to those from western Mexico cannot be attributed to their higher total iron concentrations, because a similarly low Fe^{3+}/Fe^{T} ratio of 23% was obtained for the phlogopite separates from the Leucite Hills wyomingite. Although two textural types are represented by the Uganda samples, one inferred to be metasomatic and the other magmatic, the mineral chemistry of the micas including Fe^{3+}/Fe^{T} ratios is indistinguishable. Unfortunately, there is no means by which to evaluate the oxygen fugacity of these xenoliths.

There are several possible exchange reactions between phlogopite (or biotite) and a host silicate melt that involve ferric iron. These include: $Fe^{3+}(Al)_{-1}$, $Fe^{3+}_2(MgTi)_{-1}$, $Fe^{3+}_2(MgSi)_{-1}$, $AlFe^{3+}(MgSi)_{-1}$, $AlFe^{3+}(MgTi)_{-1}$, $Fe^{3+}_2(Fe^{2+}Ti)_{-1}$, $Fe^{3+}_2(Fe^{2+}Si)_{-1}$, $AlFe^{3+}(Fe^{2+}Si)_{-1}$, $AlFe^{3+}(Fe^{2+}Ti)_{-1}$ and $Fe^{3+}O^{2-}(Fe^{2+}OH^{1-})_{-1}$. Examination of the mineral formulae in Table 2 leads to the conclusion that the largest compositional differences between the Mascota and Uganda micas do not include OH, but rather Mg, Fe^{3+}, Fe^{2+} and Ti. The principal differences in composition are best expressed in terms of the following two exchange reactions: $Mg^{2+}(Fe^{2+})_{-1}$ and $Fe^{3+}_2(Fe^{2+}Ti)_{-1}$. Thus, it is likely that the host magmas that crystallized the Mascota phlogopites had higher MgO and Fe_2O_3 concentrations relative to the Uganda magmas, which in turn were enriched in FeO and TiO_2. These differences are consistent with the fact that OIB-related magmas have long been recognized to contain higher FeO_T and TiO_2 relative to arc-related magmas (Fitton et al. 1991). Moreover, the higher Fe_2O_3 contents in the Mascota magmas suggest that they were characterized by higher oxygen fugacities.

Variation in X_{OH} with tectonic setting

Just as the Fe^{3+}/Fe^{T} ratios of the phlogopite and biotite phenocrysts should be related to the f_{O_2} of their respective host liquids, the hydroxyl contents of the biotite phenocrysts should also be correlated with the a_{H_2O} in the magma. For the samples analyzed in this study, the deficiency in the hydroxyl site caused by the less than ideal quantities of water (4-OH) is only in part made up by F and Cl, with the remainder assumed to be filled by oxygen. Although the concentration OH, F and Cl in the hydroxyl are directly related to the fugacities of these respective components in the host melt, this is not the case for oxygen. The amount of oxygen in the hydroxyl site need not be related to oxygen fugacity (the measure of f_{O_2} is in the ferric-ferrous ratio and not the number of oxygens in a melt), and instead correlates inversely with the amount of water, fluorine and chlorine occupying this site.

The hydroxyl contents of the mica samples analyzed in this study (Fig. 4b) show no variations between different tectonic settings. Nor is there any correlation between the OH contents and the Fe^{3+}/Fe^{T} ratios in the micas (Fig. 4c), which confirms that magmatic f_{O_2} and f_{H_2O} are independent variables. In other words, hydrous magmas need not be oxidized. Moreover, it suggests that alkaline magmatism with an OIB-like trace element signature can be just as hydrous as subduction-related magmatism. The distinguishing feature appears not to be water activity but rather oxygen fugacity.

Element partitioning between mica and coexisting phases

Measurements of element partitioning between silicate liquids and crystallizing phases, and between two coexisting phenocrysts, provide an important tool in igneous petrology. Equilibrium partitioning of elements between phases is used to model the chemical evolution of magmas under a variety of melting and crystallization processes, and is also important to thermometry and oxybarometry calculations. Currently, there are no experimental constraints on the Mg-Fe^{2+} exchange reaction between phlogopite (or biotite) and coexisting phases such as olivine, clinopyroxene and hornblende. For example, consider the following exchange reaction:

$$\underset{\text{mica}}{1/3\,KMg_3Si_3AlO_{10}(OH)_2} + \underset{\text{olivine}}{1/2\,Fe_2SiO_4} = \underset{\text{mica}}{1/3\,KFe_3Si_3AlO_{10}(OH)_2} + \underset{\text{olivine.}}{1/2\,Mg_2SiO_4} \quad (3)$$

The ideal contribution to the equilibrium constant is:

$$K^{Mg/Fe^{2+}}_{D(ol-phl)} = \frac{(X_{Mg}/X_{Fe^{2+}})^{ol}}{(X_{Mg}/X_{Fe^{2+}})^{phl}} \quad (4)$$

On the basis of complete analyses of biotite, hornblende and clinopyroxene (including direct measurements of FeO and FeO^T; Table 1), values were calculated for $K^{Mg/Fe^{2+}}_D$ of phlogopite-olivine, biotite-hornblende and phlogopite-augite pairs. Values for $K^{Mg/Fe^{2+}}_{D\,(ol-phl)}$ (+ 2s errors) of 0.12 + 0.12, 0.26 + 0.14 and 0.09 + 0.12

were obtained for samples Mas-3a, -4 and -11, respectively, indicating that $X_{Mg}/X_{Fe^{2+}}$ ratios are much higher in phlogopite than in coexisting olivine. The large relative errors in the derived values of $K_{D(ol-phl)}^{Mg/Fe^{2+}}$ are caused by low ferrous iron concentrations in the phlogopite phenocrysts. Values for $K_{D(hbd-bt)}^{Mg/Fe^{2+}}$ of 1.22 + 0.10 and 0.73 + 0.08 were calculated for samples SN-31 and SN-161. The range in published values of $K_{D(hbt-bt)}^{Mg/Fe^{2+}}$ for coexisting biotite and hornblende from a variety of plutonic rocks is 0.9–1.4 and appears to be correlated with the concentration of tetrahedral Al in the hornblende (Speer 1984). Our data are broadly consistent with this trend and indicate that values of $K_{D(hbt-bt)}^{Mg/Fe^{2+}}$ can vary from 0.7 to 1.4. A $K_{D(cpx-phl)}^{Mg/Fe^{2+}}$ value of 1.15 + 0.12 was obtained for the phlogopite-clinopyroxenite sample B37-5 from Uganda, indicating similar $X_{Mg}/X_{Fe^{2+}}$ ratios between equilibrium pairs of phlogopite and clinopyroxene. It was not possible to obtain a pure augite separate from any of the minette samples because most of the augite occurs as small microphenocrysts. However, if a $K_{D(cpx-phl)}^{Mg/Fe^{2+}}$ value of 1.15 is employed, the Fe^{3+}/Fe^{T} ratio in the Mas-141 augite microphenocrysts is 86%. It is likely, however, that values for $K_{D(cpx-phl)}^{Mg/Fe^{2+}}$ are as variable as those for $K_{D(hbd-bt)}^{Mg/Fe^{2+}}$. Values for $K_{D(cpx-phl)}^{Mg/Fe^{2+}}$ of 0.7 and 1.4 applied to Mas 141 lead to Fe^{3+}/Fe^{T} ratios of 78% and 89%, respectively, in the augite microphenocrysts. Therefore, within a possible range of $K_{D(cpx-phl)}^{Mg/Fe^{2+}}$ values (¥ 0.7–1.4), a substantial concentration of the esseneite component ($CaFe^{3+}AlSiO_6$) occurs in the Mascota clinopyroxenes, which is consistent with their lemon yellow color in plane-polarized light and slight pleochroism (Cosca and Peacor 1987).

Calculated $K_{D(hbd-bt)}^{F/OH^-}$ values of for biotite-hornblende pairs in samples SN-31 and SN-161 were also calculated, but have large errors (0.80 + 1.11 and 1.63 + 2.76) because of the low F contents (<0.20 wt%; Table 1) in all four phases.

Large variations in dD: a reflection of exchange with meteoric water

There has been considerable debate as to whether the large variations found in the D/H ratio of mantle-derived magmas and xenoliths are inherited from the mantle itself (e.g., Sheppard and Epstein 1970), or if secondary exchange processes have altered the primary mantle isotopic signatures (Kyser and O'Neil 1984). The biotite- and phlogopite-clinopyroxenite xenoliths from the East African Rift have dD values from −70 to −49‰, which overlap those believed to represent "primary" mantle dD (Craig and Lupton 1976; Satake and Matsuda 1979; Guy et al. 1992). Boettcher and O'Neil (1980) recommend dD = −80 to −60‰ for pristine mantle. Minor amounts of volatilization may account for some of this variation. In addition, small-scale hydrogen isotope heterogeneity also may be indicated for the East African Rift mantle. The presence of Pb isotope heterogeneity in the East African Rift mantle (<1 m) was also inferred from analyses of biotite and phlogopite separates from the same samples employed in this study (Davies and Lloyd 1986).

The dD values of phlogopite phenocrysts from the western Mexico minettes vary by almost a 100‰ for flows and cones within 20 km of each other, erupting over a 475 ky interval. Of all the dD values published for mantle minerals (Sheppard and Epstein 1970; Kuroda et al. 1975, 1977; Sheppard and Dawson 1975; Boettcher and O'Neil 1980; Kyser and Stern 1988; Deloule et al. 1991), none have been as low as those of some of the phlogopite phenocrysts from western Mexico. The effect of crystal fractionation plays only a negligible role in producing variations in the D/H ratio of minerals at the crystallization temperatures of these minettes (¥ 1100–1200°C), probably less than 10‰ (Suzuoki and Epstein 1976; Kyser and Stern 1988). Likewise, differing degrees of partial melting will not contribute to the variation in D/H ratio between different melts of an isotopically homogeneous source region, and therefore between phlogopite phenocrysts crystallizing from these melts.

If the large variation in dD for phlogopite phenocrysts from the minette lavas were caused by magmatic degassing (Nabelek et al. 1983; Taylor et al. 1983; Kyser and O'Neil 1984; Newman et al. 1988), volatilization of hydrogen (as H_2) accompanied by dehydroxylation (Eq. 1) would require almost 100 per cent loss of magmatic water, which is unrealistic given the stability of the hydrous phenocrysts. Magmatic degassing of H_2O is equally unlikely; the isotopic heterogeneity found in the phlogopite separate splits from Mas-3a (dD = −137‰ and −103‰) also requires almost 100 per cent loss of magmatic water, yet the phlogopite phenocrysts in this sample are free of reaction rims (Fig. 1a, b).

A possible explanation for the large variation in dD values is isotopic heterogeneity in the sub-arc mantle of western Mexico. Although subduction-related lavas generally have relatively high dD values (Poreda 1985; Dobson and O'Neil 1987; Fig. 4a), altered oceanic crust with dD values as low as −145‰ has been observed in drill cores down to 800 m depth (Hoernes and Friedrichsen 1979a, b; Friedrichsen and Hoernes 1980; Marumo et al. 1980; Friedrichsen 1984; Sakai et al. 1990). Subduction of this material and release of water with variable D/H ratios into the mantle wedge could result in a mantle source region for arc magmas that is heterogeneous with respect to deuterium. However, the $d^{18}O$ values for the Mascota phlogopites are consistent with normal mantle values and strongly argue against isotopic heterogeneity in the mantle as an explanation for the anomalous and variable phlogopite dD values.

The most likely scenario is that the Mascota phlogopite phenocrysts attained their light hydrogen isotope composition through exchange with meteoric water, sufficient to alter their dD but not their $d^{18}O$ values, analogous to exchange between a cooling pluton and water in meteoric-hydrothermal systems (Taylor 1977; Criss and Taylor 1986). For example, Mas-3a and -11 (two lava flows that erupted side by side, but 400 ky

apart) have phlogopite phenocrysts with distinctly different dD values and yet have similar $d^{18}O$ values as well as almost identical whole rock compositions, phenocryst assemblages and phenocryst compositions (including the ferric-ferrous ratio and hydroxyl content). These two lavas are remarkable for their similar compositions in every aspect except their D/H ratio and their age. It may be important that the sample with the more "normal" dD value (Mas-11) erupted first, whereas the sample with the anomalously low dD value (Mas-3a) erupted 400 thousand years later.

One probable scenario is that during cooling and crystallization of the magma body that supplied the Mas-11 eruption, exchange with meteoric water occurred to an extent sufficient to offset the D/H ratio but insufficient to affect the $d^{18}O$ values. This scenario is plausible because even hydrous magmas contain far more oxygen than hydrogen, and therefore are more sensitive to changes in their hydrogen vs oxygen isotope ratios. After exchange of meteoric water sufficient to alter the D/H ratio, the magma must have been reheated to a temperature similar to that at the time of the eruption of Mas-11, probably because of the intrusion of another magma body close by. Eruption of the reheated magma would give rise to a lava of nearly identical bulk composition to Mas-11. The most remarkable feature, however, is that the phlogopite phenocrysts in both Mas-3a and Mas-11 have such similar hydroxyl contents and ferric-ferrous ratios, strongly suggesting that the exchange of meteoric water did not also change the oxygen fugacity or water fugacity of the host magma.

Interaction with meteoric water sufficient to alter the stable isotope composition of a magma and its phenocrysts, without also changing the major element composition or oxygen fugacity of the system is not unprecedented; an example is the rhyolite magmas of the Yellowstone volcanic field. Hildreth et al. (1984) suggested that profound modification of $d^{18}O$ values from +7.2, +5.8 and +6.3‰ (representing the three major ashflow eruptions) down to 1‰ (for the earliest of the postcaldera rhyolites) occurred by exchange with meteoric water. However, as pointed out by Carmichael (1991), the maximum variation in f_{O_2} (determined by two Fe-Ti oxides) between rhyolites of drastically different oxygen isotope values is within 0.5 log units. Thus it appears that exchange with meteoric water sufficient to alter $d^{18}O$ values need not substantially affect magmatic f_{O_2}. A similar process may be occurring with the Mexican minette magmas, where the anomalously low dD values reflect exchange of meteoric water but leads to no corresponding changes in the magmatic intensive variables as reflected in the phlogopite phenocryst hydroxyl content, ferric-ferrous ratio or host magma major element composition.

Acknowledgements Gareth Davies is thanked for providing the Ugandan samples, and Ian Carmichael is thanked for providing the FeO analyses on the mineral separates. Eric Essene provided numerous helpful discussions regarding mineral formula normalization schemes and direct analyses of oxygen. Carl Henderson gave invaluable assistance with the electron microprobe (funded by EAR 82–12764). Thorough and constructive reviews of this paper by Eric Essene, Ian Carmichael, Youxue Zhang, Bob Luth and an anonymous reviewer significantly improved this manuscript. Support was provided in part by Sigma Xi and Scott Turner awards to S. N. Feldstein, and NSF grants 92–19070 to R. A. Lange and 92–05314 to J. R. O'Neil.

Appendix. Standards employed for electron microprobe analyses of biotite

Element	Standard	
Al	Andalusite	U. of Michigan collection
Ba	Sanbornite	U. of Michigan collection
Ca	Aluminous diopside megacryst	Southeast Australia; U. of Michigan collection
Cl	Alforsite	Synthesized by C. Prewitt
Cr	Uvarovite	Synthesized by D. Perkins
F	Fluorotopaz	Topaz Mountain, Utah; U. of Michigan collection
Fe	Ferrosilite	Synthesized by S. Bohlen
K	Adularia	St. Gotthard; U. of Michigan collection
Mg	Marjalahti olivine	Meteorite; U. of Chicago collection
Mn	Rhodonite	Broken Hill, Australia; U. of Michigan collection
Na	Albite	Tiburon, California; U. of Michigan collection
Ni	NiS	Synthesized at U. Toronto
O	Hornblende megacryst	Kakanui, New Zealand; U. of Michigan collection
Si	Aluminous diopside megacryst	Southeast Australia; provided by A.J. Irving
Ti	Geikielite	Synthesized by E. Essene

References

Afifi AM, Essene EJ (1988) MINFILE: a microcomputer program for storage and manipulation of chemical data on minerals. Am Mineral 73: 446–448

Arima M, Edgar AD (1983) High pressure experimental studies on a katungite and their bearing on the genesis of the potash-rich magma of the west branch of the African rift. J Petrol 24: 166–187

Armstrong JT (1988) Accurate quantitative analysis of oxygen and nitrogen with a W/Si multilayer crystal. In: Newbury DE (ed) Microbeam analysis 1988. San Francisco Press, San Francisco, pp 301–304

Atwater TM (1970) Implications for the Cenozoic tectonic evolution of western North America. Geol Soc Am Bull 81: 3518–3536

Bastin GF, Heijligers HJM (1989) Quantitative EMPA of oxygen. In: Russel PE (ed) Microbeam analysis 1989. San Francisco Press, San Francisco, pp 207–210

Boettcher Al, O'Neil JR (1980) Stable isotope, chemical, and petrographic studies of high-pressure amphiboles and micas: evidence for metasomatism in the mantle source regions of alkali basalts and kimberlites. Am J Sci 280-A:594–621

Bohlen SR, Peacor DR, Essene EJ (1980) Crystal chemistry of a metamorphic biotite and its significance in water barometry. Am Mineral 65: 55–62

Borthwick J, Harmon RS (1982) A note regarding ClF_3 as an alternative to BrF_5 for oxygen isotope analysis. Geochim Cosmochim Acta 46: 1665–1668

Carmichael ISE (1967) The mineralogy and petrology of the volcanic rocks from the Leucite Hills, Wyoming. Contrib Mineral Petrol 15: 24–66

Carmichael ISE (1991) The redox states of basic and silicic magmas: a reflection of their source regions? Contrib Mineral Petrol 106: 129–141

Carmichael ISE, Lange RA, Luhr JF (1996) Quaternary minettes and associated lavas of Mascota, western Mexico: a consequence of plate extension above a subduction- modified mantle wedge. Contrib Mineral Petrol 124 (in press)

Chandra U, Lokanathan S (1982) A Mössbauer study of the effect of heat treatment on biotite micas. J Phys D 15: 2331–2340

Cosca MA, Peacor DR (1987) Chemistry and structure of esseneite ($CaFe^{3+}AlSiO_6$), a new pyroxene produced by pyrometamorphism. Am Mineral 72: 148–156

Cosca MA, Essene EJ, Bowman JR (1991) Complete chemical analyses of metamorphic hornblendes: implications for normalizations, calculated H_2O activities and thermobarometry. Contrib Mineral Petrol 108: 472–484

Craig H, Lupton JE (1976) Primordial neon, helium, and hydrogen in oceanic basalts. Earth Planet Sci Lett 31: 369–385

Criss RE, Taylor HP (1986) Meteoric-hydrothermal systems. In: Valley JW, Taylor HP, O'Neil JR (eds) Stable isotopes (Reviews in Mineralogy vol. 16). Mineralogical Society of America, Washington DC, pp 373–424

Cross W (1897) The igneous rocks of the Leucite Hills and Pilot Butte, Wyoming. Am J Sci 4: 115–141

Davies GR, Lloyd FE (1986) Pb-Sr-Nd isotope and trace element data bearing on the origin of the potassic subcontinental lithosphere beneath southwest Uganda. Proceedings, 4th International Kimberlite Conference, Perth, Australia, pp 784–794

Deer WA, Howie RA, Zussman J (1962) Rock-forming minerals. Vol 3: Sheet silicates. Longmans, London

Deloule E, Albarede F, Sheppard SMF (1991) Hydrogen isotope heterogeneities in the mantle from ion probe analysis of amphiboles from ultramafic rocks. Earth Planet Sci Lett 105: 543–553

Dixon JE, Clague DA, Stolper EM (1991) Degassing history of water, sulfur, and carbon in submarine lavas from Kilauea Volcano, Hawaii. J Geol 99: 371–394

Dobson PF, O'Neil JR (1987) Stable isotope compositions and water contents of boninite series volcanic rocks from Chichijima, Bonin Islands, Japan. Earth Planet Sci Lett 82: 75–80

Doelter C (1917) Handbuch der Mineralchemie. Verlag von Theodor Steinkopff, Dresden

Dyar MD (1988) Direct evidence of hydronium substitution in biotite. Geol Soc Am Abstr Prog 20:A102

Dyar MD (1990) Mössbauer spectra of biotite from metapelites. Am Mineral 75: 656–666

Dyar MD, Burns RG (1986) Mössbauer spectral study of ferruginous one-layer trioctahedral micas. Am Mineral 71: 951–961

Dyar MD, Colucci MT, Guidotti CV (1991) Forgotten major elements: hydrogen and oxygen variation in biotite from metapelites. Geology 19: 1029–1032

Dymek RF (1983) Titanium, aluminum and interlayer cation substitution in biotite from high-grade gneisses, West Greenland. Am Mineral 68: 880–899

Feldstein SN (1997, expected) Melting processes and the generation of chemical variability in terrestrial and extraterrestrial magmas. PhD thesis, Univ Michigan, Ann Arbor, Michigan

Ferrow E (1987) Mössbauer and X-ray studies on the oxidation of annite and ferriannite. Phys Chem Mineral 14: 270–275

Foley SF, Taylor WR, Green DH (1986) The role of fluorine and oxygen fugacity in the genesis of the ultrapotassic rocks. Contrib Mineral Petrol 94: 183–192

Foster M (1960) Interpretation of trioctahedral micas. US Geol Surv Prof Paper 354-B

Friedrichsen H (1984) Strontium, oxygen, and hydrogen isotope studies on primary and secondary minerals in basalts from the Costa Rica rift, Deep Sea Drilling Project Hole 504B, Leg 83. Initial Rep Deep Sea Drill Proj 83: 289–295

Friedrichsen H, Hoernes S (1980) Oxygen and hydrogen isotope exchange reactions between seawater and oceanic basalts from Leg 51 through 53. Initial Rep Deep Sea Drill Proj 51–53: 1177–1180

Gerlach TM (1993) Oxygen buffering of Kilauea volcanic gases and the oxygen fugacity of Kilauea basalt. Geochim Comsochim Acta 57: 795–814

Goldstein JI, Newbury DE, Echlin P, Joy DC, Fiori C, Lifshin E (1981) Scanning electron microscopy and X-ray microanalysis. Plenum Press, New York

Goldstein JJ, Choi SK, van Loo FJJ, Heijligers HJM, Dijkstra JM, Basin GF (1991) The influence of surface oxgyen contamination of bulk EMPA of oxygen in ternary titanium-oxygen compounds. In: Howitt DG (ed) Microbeam analysis 1991. Plenum Press, New York, pp 57–58

Graham CM, Viglino JA, Harmon RS (1987) Experimental study of hydrogen exchange between aluminous chlorite and water and of hydrogen diffusion in chlorite. Am Mineral 72: 566–579

Guidotti CV, Dyar MD (1991) Ferric iron in metamorphic biotite and its petrologic and crystallochemical implications. Am Mineral 76: 161–175

Guttler B, Nieman W, Redfern SAT (1989) EXAFS and XANES spectroscopy study of the oxidation deprotonation of biotite. Mineral Mag 53: 591–602

Guy C, Schott J, Destrigneville C, Chiappini R (1992) Low-temperature alteration of basalt by interstitial seawater, Mururoa, French Polynesia. Geochim Cosmochim Acta 56: 4169–4189

Hawkesworth CJ, Vollmer R (1979) Crustal contamination versus enriched mantle: $^{143}Nd/^{144}Nd$ and $^{87}Sr/^{86}Sr$ evidence from the Italian volcanics. Contrib Mineral Petrol 69: 151–165

Hewitt DA, Abrecht J (1986) Limitations on the interpretation of biotite substitutions from chemical anlayses of natural samples. Am Mineral 71: 1126–1128

Hildreth W, Christiansen R, O'Neil J (1984) Catastrophic isotopic modification of rhyolitic magma at times of caldera subsidence, Yellowstone Plateau volcanic field. J Geophys Res 89: 8339–8369

Hoernes S, Friedrichsen H (1979a) Oxygen- and hydrogen-isotope and trace element investigations on rocks of DSDP Hole 395A Leg 45. Initial Rep Deep Sea Drill Proj 45: 541–550

Hoernes S, Friedrichsen H (1979b) $^{18}O/^{16}O$ and D/H investigation on basalts of Leg 46. Initial Rep Deep Sea Drill Proj 46: 253–255

Hogg CS, Mead RE (1975) A Mössbauer study of thermal decomposition of biotites. Mineral Mag 40: 79–88

Holdaway MJ (1980) Chemical formulae and activity models for biotite, muscovite, and chlorite applicable to pelitic metamorphic rocks. Am Mineral 65: 711–719

Kuehner SM, Edgar AD, Arima M (1981) Petrogenesis of the ultrapotassic rocks from the Leucite Hills. Am Mineral 66: 663–677

Kuroda Y, Suzuoki T, Matsuo S, Aoki K (1975) D/H ratios of the coexisting phlogopite and richterite from mica nodules and a peridotite in South Africa kimberlites. Contrib Mineral Petrol 52: 315–318

Kuroda Y, Suzuoki T, Matsuo S (1977) Hydrogen isotope composition of deep-seated water. Contrib Mineral Petrol 60: 311–315

Kyser TK, O'Neil JR (1984) Hydrogen isotope systematics of submarine basalts. Geochim Cosmochim Acta 48: 2123–2133

Kyser TK, Stern CR (1988) Oxygen and hydrogen isotope systematics in alkali basalts and mantle xenoliths from the Patagonian Plateau. Geol Soc Am Abstr Prog 20:A6

Lange RA, Carmichael ISE (1989) Ferric-ferrous equilibria in Na_2O-FeO-Fe_2O_3-SiO_2 melts: effects of analytical techniques on derived partial molar volumes. Geochim Cosmochim Acta 53: 2195–2204

Lange RA, Carmichael ISE (1991) A potassic volcanic front in western Mexico: the lamprophyric and related lavas of San Sebastian. Geol Soc Am Bull 103: 928–940

Lange RA, Carmichael ISE (1996) The Aurora volcanic field, California-Nevada: oxygen fugacity constraints on the development of andesitic magma. Contrib Mineral Petrol (in press)

Lange RA, Carmichael ISE, Renne PR (1993) Potassic volcanism near Mono basin, California: evidence for high water and oxygen fugacities inherited from subduction. Geology 21: 949–952

Lloyd F (1972) The petrogenesis of strongly alkaline mafic lavas and nodules from southwest Uganda. PhD thesis, University of Reading

Lloyd FE (1981) Upper mantle metasomatism beneath a continental rift: clinopyroxenes in alkali mafic lavas and nodules from southwest Uganda. Mineral Mag 44: 315–323

Lloyd FE (1987) Characterization of mantle metasomatic fluids in spinel lherzolites and alkali clinopyroxenites from the west Eifel and southwest Uganda. In: Menzies MA, Hawkesworth CJ (ed) Mantle metasomatism. Academic Press, London, pp 472

Lloyd FE, Bailey DK (1975) Light element metasomatism of the continental mantle: the evidence and the consequences. Phys Chem Earth 9: 389–410

Lloyd FE, Arima M, Edgar AD (1985) Partial melting of a phlogopite-clinopyroxenite nodule from southwest Uganda: an experimental study bearing on the origin of highly potassic continental rift volcanic. Contrib Mineral Petrol 91: 321–329

Lloyd FE, Nixon PH, Hornung G, Condliffe E (1987) Regional K-metasomatism in the mantle beneath the west branch of the east African rift: alkali clinopyroxenite xenoliths in highly potassic magmas. In: Nixon P (ed) Mantle xenoliths. John Wiley and Sons, New York, pp 641–659

Luhr JF, Allan JF, Carmichael ISE, Nelson SA, Hasenaka T (1989) Primitive calc-alkaline and alkaline rock types from the western Mexican volcanic belt. J Geophys Res 94: 4515–4530

MacDowell FW (1966) Potassium argon dating of Cordilleran intrusives. PhD thesis, University of Colorado

Malahoff A, Moberly RJ (1968) Effects of structure on the gravity field of Wyoming. Geophysics 33: 781–804

Marumo K, Nagasawa K, Kuroda Y (1980) Mineralogy and hydrogen isotope geochemistry of clay minerals in the Ohnuma geothermal area, northeastern Japan. Earth Planet Sci Lett 47: 255–262

Mathez EA (1984) Influence of degassing on oxidation states of basaltic magmas. Nature 310: 371–375

Nabelek PI, O'Neil JR, Papike JJ (1983) Vapor exsolution as a controlling factor in hydrogen isotope variation in granitic rocks: the Notch Peak granitic stock, Utah. Earth Planet Sci Lett 66: 137–150

Newman S, Epstein S, Stolper E (1988) Water, carbon dioxide, and hydrogen isotopes in glasses from the ca. 1340 A.D. eruption of the Mono Craters, California: constraints on degassing phenomena and initial volatile content. J Volcanol Geotherm Res 35: 75–96

Nockolds JR (1947) The relation between chemical composition and paragenesis in the biotite micas of igneous rocks. Am J Sci 245: 401–420

Poreda R (1985) Helium-3 and deuterium in back-arc basalts: Lau Basin and the Mariana Trough. Earth Planet Sci Lett 73: 244–254

Rancourt DG, Tume P, Lalond AE (1993) Kinetics of the $(Fe^{2+} + OH^-)_{mica} = (Fe^{3+}+O^{2-})_{mica} + H$ oxidation reaction in bulk single-crystal biotite studies by Mössbauer spectroscopy. Phys Chem Mineral 20: 276–284

Rimsaite J (1970) Structural formulae of oxidized and hydroxyl-deficient micas and decomposition of the hydroxyl group. Contrib Mineral Petrol 25: 225–240

Rutherford MJ, Hill PM (1993) Magma ascent rates from amphibole breakdown: an experimental study applied to the 1980–1986 Mount St. Helens eruption. J Geophys Res 98: 19667–19685

Sakai R, Kusakabe M, Noto M, Ishii T (1990) Origin of water responsible for serpentinization of the Izu-Ogasawara-Mariana forearc seamounts in view of hydrogen and oxygen isotope ratios. Earth Planet Sci Lett 100: 291–303

Sanz J, Gonzalez-Carreno T, Gancedo R (1983) On dehydroxylation mechanisms of a biotite in vacuo and in oxygen. Phys Chem Mineral 9: 14–18

Satake J, Matsuda J (1979) Strontium and hydrogen isotope geochemistry of fresh and metabasalt dredged from the mid-Atlantic ridge. Contrib Mineral Petrol 70: 153–157

Sato M (1978) Oxygen fugacity of basaltic magmas and the role of gas-forming elements. Geophys Res Lett 5: 447–449

Schumacher JC (1991) Empirical ferric iron corrections: necessity, assumptions, and effects on selected geothermobarometers. Mineral Mag 55: 3–18

Sheppard SMF, Dawson JB (1975) Hydrogen, carbon and oxygen isotope studies of megacrysts and matrix minerals from Lesothan and South African kimberlites. Phys Chem Earth 9: 747–763

Sheppard SMF, Epstein S (1970) D/H and $^{18}O/^{16}O$ ratios of minerals of possible mantle or lower crustal origin. Earth Planet Sci Lett 9: 232–239

Speer JA (1984) Micas in igneous rocks. In: Bailey SW (ed) Micas (Reviews in Mineralogy vol. 13). Mineralogical Society of America, Washington DC, pp 299–356

Suzuoki T, Epstein S (1976) Hydrogen isotope fractionation between OH-bearing minerals and water. Geochim Cosmochim Acta 40: 1229–1240

Taylor BE, Eichelberger JC, Westrich HR (1983) Hydrogen isotopic evidence of rhyolitic magma degassing during shallow intrusion and eruption. Nature 306: 541–545

Taylor HP Jr (1977) Water/rock interaction and the origin of H_2O in granitic batholiths. J Geol Soc London 133: 509–588

Thibault Y, Holloway JR (1994) Solubility of CO_2 in a Ca-rich leucitite: effects of pressure, temperature, and oxygen fugacity. Contrib Mineral Petrol 116: 216–224

Tikhomirova VI, Konilov AN, Koshemchuk SK (1989) The degree of oxidation of iron in synthetic iron-magnesian biotites. Mineral Petrol 41: 41–52

Vedder W, Wilkins RWT (1969) Dehydroxylation and rehydroxylation, oxidation and reduction of micas. Am Mineral 54: 482–509

Vennemann TW, O'Neil JR (1993) A simple and inexpensive method of hydrogen isotope and water analyses of minerals and rocks based on zinc reagent. Chem Geol 103: 227–234

Vennemann TW, Smith HS (1990) The rate and temperature of reaction of ClF_3 with silicate minerals and their relevance to oxygen isotope analysis. Chem Geol 86: 83–88

Vollmer R, Odgen P, Schilling JG, Kingsley RH, Waggoner DG (1984) Nd and Sr isotopes in ultrapotassic volcanic rocks from the Leucite Hills, Wyoming. Contrib Mineral Petrol 87: 359–368

Wallace PJ, Carmichael ISE (1989) Minette lavas and associated leucitites from the western front of the Mexican volcanic belt: petrology, chemistry, and origin. Contrib Mineral Petrol 103: 470–492

Wilson AD (1960) The micro-determination of ferrous iron in silicate minerals by a volumetric and colorimetric method. Analyst 85: 823–827

Winchell AN (1935) The biotite system. Am Mineral 20: 773–779

Zoback ML, Anderson RE, Thompson GA (1981) Cainozoic evolution of the state of stress and style of tectonism of the Basin and Range province of the western United States. Phil Trans R Soc Lond Ser A 300: 407–434